ELSEVIER

Available online at www.sciencedirect.com

ScienceDirect

Polymer 48 (2007) 4034–4040

polymer

www.elsevier.com/locate/polymer

In situ grafting of carboxylic acid-terminated hyperbranched poly(ether-ketone) to the surface of carbon nanotubes

Ja-Young Choi [a], Sang-Wook Han [a], Wan-Soo Huh [b], Loon-Seng Tan [c], Jong-Beom Baek [a,*]

[a] *School of Chemical Engineering, Chungbuk National University, Cheongju, Chungbuk 361-763, South Korea*
[b] *Department of Chemical and Environmental Engineering, Soongsil University, Seoul 156-743, South Korea*
[c] *Polymer Branch, Materials & Manufacturing Directorate, AFRL/MLBP, Air Force Research Laboratory,*
Wright-Patterson Air Force Base, Dayton, OH 45433-7750, USA

Received 9 March 2007; received in revised form 24 April 2007; accepted 26 April 2007
Available online 7 May 2007

Abstract

Carboxylic acid-terminated hyperbranched poly(ether-ketone)s (HPEKs) were successfully grafted onto the surfaces of single-walled carbon nanotube (SWNT) and multi-walled carbon nanotube (MWNT) to afford HPEK-*g*-SWNT and HPEK-*g*-MWNT nanocomposites. They were prepared via *in situ* polymerization of 5-phenoxyisophthalic acid as an AB_2 monomer for the HPEK in the presence of SWNT or MWNT in polyphosphoric acid (PPA)/phosphorous pentoxide (P_2O_5) medium. The resultant nanocomposites were homogeneously dispersed in various common polar aprotic solvents as well as in concentrated ammonium hydroxide. The experimental results from Soxhlet extraction, solubility enhancement, elemental analysis (EA), thermogravimetric analysis (TGA), and scanning electron microscopy (SEM) provided clear evidences for grafting of hyperbranched polymers onto the surfaces of corresponding CNT's. Achieving enhanced solubility of CNT's in common organic solvents via the functionalization of CNT's is a key step for CNT's to be used in various application-specific purposes. The results could potentially envision to the area of CNT researches via the efficient introduction of three-dimensional globular dendritic macromolecules as increasing solubility, available multi-functionality, reactivity, processability, and also biocompatibility.

Keywords: Carbon nanotubes; Hyperbranched poly(ether-ketone); Polyphosphoric acid

---

1. Introduction

Carbon-based nano-structured materials such as single-walled carbon nanotubes (SWNT's), multi-walled carbon nanotubes (MWNT's) and multi-walled carbon nanofibers (MWNF's) have attracted a lot of attention due to their unique properties for a wide variety of potential applications such as nanocomposites, electronic devices, field emission display and hydrogen storage, and other fields of materials science [1]. When they are used as reinforcing additives for nanocomposites, they could deliver their outstanding properties to support matrices such as polymers [2–7], ceramics [8,9], and even low melting metals [10,11]. The resultant nanocomposites would possibly possess enhanced properties providing various potential applications for areas, which require affordable, light-weight, multifunctional materials. In order to achieve maximum enhanced properties through such nanoscale additives, SWNT's are the best candidate for the nanocomposites because of the highest length to diameter ratio and relatively lower defects. Nonetheless, MWNT's are relatively attractive from the standpoints of lower cost than SWNT's and better aspect ratio than MWNF's. However, two fundamental issues must be considered when dealing with carbon nanotubes (CNT's). They are the aspect ratio mainly depending upon the state of dispersion in matrix and interfacial adhesion between additives and matrix. Thus, there have been many efforts to provide homogeneous dispersion of CNT's in various matrix materials via physical [12–21], chemical [7,22–27], or combined approaches [20,28,29]. However, structural damages to CNT's, which were resulted from the treatment

---

* Corresponding author. Tel.: +82 43 261 2489; fax: +82 43 262 2380.
E-mail address: jbbaek@chungbuk.ac.kr (J.-B. Baek).

0032-3861/$ - see front matter © 2007 Elsevier Ltd. All rights reserved.
doi:10.1016/j.polymer.2007.04.073

conditions such as power levels, exposure times, and temperatures, had occurred in many cases [30]. Even after homogeneous CNT dispersion has been achieved, the immediate issue is realizing strong interfacial adhesion between CNT and matrix. Furthermore, an additional issue for SWNT is persisting impurities such as metallic catalysts and carbonaceous fragments (amorphous and crystalline carbon beads). To remove those impurities, there have been many reports on the purification with strong acids. They can oxidize and decompose catalysts as well as carbonaceous impurities, and also damage CNT's such as side-wall opening and breaking [31,32]. Furthermore, SWNT's revealed to be by far the most vulnerable due to their fragile structure consisting of a single wall. The most recent report is clearly demonstrating that previous reports claiming side-wall functionalization of the SWNT's with carboxylic acid groups in nitric acid should be reconsidered [33].

To achieve better dispersion of carbon nanomaterials into relevant matrices, the introduction of hyperbranched polymers onto the surface of CNT has been the subject of considerable interest. Their unique highly branched structures and available surface multi-functionalities offer unusual properties such as low viscosity and enhanced solubility [34–37]. After covalent attachment of three-dimensional globular hyperbranched polymeric molecules to the side-walls of CNT's, the resultant hyperbranched polymer grafted carbon nanotube (HBP-*g*-CNT) nanocomposites potentially expected to display both enhanced dispersion and interfacial interaction. The former would be originated from impeding the lateral interaction between CNT's when hyperbranched polymers grafted to the surfaces of them. In addition, the improved solubility nature of hyperbranched polymer compared to its linear analog would further help their dispersion. The latter is enhanced by the topological roughness contributed from the broad size distribution of hyperbranched macromolecules. Furthermore, numerous periphery surface groups and fractal molecular architecture of rigid hyperbranched polymers could provide additional chemical interactions and mechanical inter-locking between HBP-*g*-CNT nanocomposite and supporting matrix.

In this regards, we have developed facile synthesis of linear and hyperbranched PEK's in poly(phosphoric acid)/phosphorous pentoxide (PPA/P_2O_5; 1/4, w/w) medium [38,39]. This approach has been further extended to grafting of linear and hyperbranched PEK's onto carbon nanomaterials [40–45].

In the light of the above we have experienced in both areas of HBP and CNT, this paper would like to report one of our continuous efforts to the important progress in the field of CNT research to achieve solubility in common organic solvents, which makes the resultant nanocomposites to be potentially useful for various applications. The proposed reaction medium acidity (PPA/P_2O_5) revealed to be mild enough not to damage CNT, but strong enough to efficiently promote the functionalization reaction. As a result, HBP-*g*-CNT nanocomposites are prepared to be potentially useful as a new class of materials with unusual properties, which are contributed from combined characteristics of three-dimensional globular hyperbranched polymers with those of CNT.

2. Experimental

2.1. Materials

All reagents and solvents were purchased from Aldrich Chemical Inc. and used as-received, unless otherwise mentioned. Both single-walled carbon nanotube (SWNT, ASA-100F with diameter of ~1.2 nm, bundle diameter of ~10 nm, and length of 5–20 nm) and multi-walled carbon nanotube (MWNT, CVD MWNT 95 with diameter of ~20 nm and length of 10–50 μm) were obtained from Iljin Nanotech Co., Ltd, Seoul, Korea [46].

2.2. Instrumentation

Infrared (IR) spectra were recorded on Jasco FT-IR 480 Plus spectrophotometer. Solid samples were imbedded in KBr disks. Elemental analyses were performed by system support at CBNU with a CE Instruments EA1110. Differential scanning calorimeter (DSC) was performed under the nitrogen atmosphere with heating and cooling rates of 10 °C/min using a Perkin–Elmer DSC7. The thermograms were obtained on powder samples after they had been heated to 300 °C and air-cooled to ambient temperature. Glass transition temperatures (T_g's) were taken as the mid-point of the baseline shift. Thermogravimetric analysis (TGA) was conducted in both nitrogen and air atmospheres with a heating rate of 10 °C/min using a Perkin–Elmer TGA7 thermogravimetric analyzer. The field emission scanning electron microscopy (FE-SEM) used in this work was LEO 1530FE.

2.3. Synthesis of AB_2 monomer (**2**)

The AB_2 monomer, 5-phenoxyisophthalic acid, was synthesized in a two-step sequence as reported in the literature [47]. The final product was recrystallized from acetic acid to afford white flakes, m.p. 310–312 °C. Anal. Calcd. for $C_{14}H_{10}O_5$: C, 65.12%; H, 3.90%; O, 30.98%. Found: C, 65.23%; H, 4.02%; O, 30.99%. FT-IR (KBr, cm^{-1}): 2986, 2828, 2565, 1692, 1587, 1489, 1466, 1420, 1321, 1280, 1250. Mass spectrum (m/e): 258 (M^+, 100% relative abundance). ^1H NMR (DMSO-d_6, δ in ppm): 7.15–7.18 (d, 2H, Ar), 7.25–7.46 (t, 1H, Ar), 7.49–7.56 (d, 2H, Ar), 7.70 (s, 2H, Ar), 8.25 (s, 1H, Ar), 13.44 (broad s, 2H, COOH). ^{13}C NMR (DMSO-d_6, δ in ppm): 119.89, 122.14, 124.50, 124.82, 130.49, 133.23, 155.52, 157.79, 166.11.

2.4. Representative procedure for in situ grafting of hyperbranched PEK's from AB_2 monomers with 10 wt% MWNT load

Into a 250 mL resin flask equipped with a high torque mechanical stirrer and nitrogen inlet and outlet, 5-phenoxyisophthalic acid (0.9 g), MWNT (0.1 g), phosphorous pentoxide (P_2O_5, 5.0 g), and polyphosphoric acid (PPA, 20 g) were charged (**3b**, Fig. 2). The mixture was stirred at 100 °C for 6 h and heated to 130 °C. When the temperature reached around 130 °C, the color of mixture turned to gray indicating that the carbonium ion ($-C^{+}{=}O$) generated to promote Friedel–Crafts reaction and the reaction mixture was still heterogeneous. After stirring 12 h at the temperature, the color of the reaction mixture was changed to deep green. It was changed to dark gray after additional 14 h later at the temperature and the phase became homogeneous with increase in visual viscosity. After cool down, distilled water was added to the reaction mixture. The dark gray chunk was isolated, collected by suction filtration, washed with 5% hydrochloric acid, and large amount of water. The product was Soxhlet extracted with water for 3 days for the complete removal of reaction medium, further extraction with methanol for additional 3 days for the removal of low molecular weight and homopolymer portions, finally freeze-dried under reduced pressure (0.05 mmHg) for 150 h to give dark gray solids. Anal. Calcd. for $C_{16.39}H_8O_4$: C, 73.20%; H, 2.98%. Found: C, 72.64%; H, 2.98%.

For the **3b**, 5-phenoxyisophthalic acid (0.9 g), SWNT (0.1 g), phosphorous pentoxide (P_2O_5, 5.0 g), and polyphosphoric acid (PPA, 20 g) were charged. The mixture was stirred at 100 °C for 6 h and heated to 130 °C. When the temperature reached around 130 °C, the color of the mixture turned to dark gray. Following the same work-up procedure for the **3a**, dark gray solids were obtained. $C_{16.39}H_8O_4$: C, 73.20%; H, 2.98%. Found: C, 69.94%; H, 3.01%.

3. Results and discussion

3.1. Synthesis of AB_2 monomer (**2**)

The AB_2 monomer (**2**), 5-phenoxyisophthalic acid, was synthesized in a two-step sequence as reported in the literature (Fig. 1) [47]. The intermediate, 1,3-dimethyl-5-phenoxybenzene (**1**) was obtained by the Ullmann reaction of potassium phenolate with 5-bromo-*m*-xylene. Compound **1** was then oxidized with potassium permanganate to from the AB_2 monomer (**2**).

3.2. Grafting of hyperbranched PEK's onto CNT from AB_2 monomers

Hyperbranched PEK grafted carbon nanotubes (SWNT and MWNT) were prepared in PPA/P_2O_5 medium at 130 °C to afford hyperbranched PEK-*g*-CNT nanocomposites (Fig. 2). For both cases of HPEK-*g*-SWNT (**3a**) and HPEK-*g*-MWNT (**3b**), the reaction mixtures were not a single phase (Fig. 3). In the beginning, the color of mixture was black due to SWNT (Fig. 3(a)). After 6 h at 130 °C, the color of the reaction mixture became light brown indicating that hyperbranched polymers were grafted to SWNT and thus homogeneously dispersed in the reaction medium. Similarly, the colors of the reaction mixture **3b** turned from black to off-gray (Fig. 3(b)).

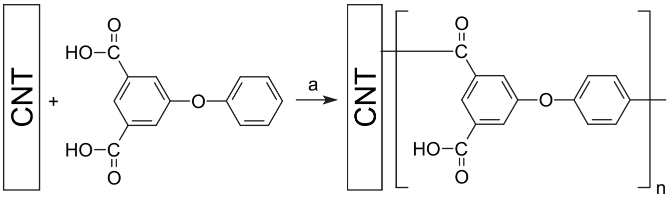

3a: Hyperbranched PEK-g-SWNT
3b: Hyperbranched PEK-g-MWNT

Fig. 2. Grafting of hyperbranched PEK's onto CNT from AB_2 monomer: PPA/P_2O_5.

The versatile reaction between vapor-grown carbon nanofiber (VGCNF) and 2,4,6-trimethylphenoxy benzoic acid was previously studied and proved that the covalent attachment of 4-substituted benzoyl moiety onto the surface of carbon nanomaterials was indeed effective in the reaction condition we had developed [40]. Linear PEK's by using AB monomers were grafted onto the surface of MWNT's [43]. The difference in this system is the covalent attachment of hyperbranched polymers from AB_2 monomer onto the surface of CNT. In this case, the monomer contains two aromatic carboxylic acids as a B-functionality that reacts with phenoxy group as well as CNT's. The probability for the covalent attachment of hyperbranched PEK to the CNT is much higher than that for linear one. It is expected to be that the chances for hyperbranched polymers prepared from AB_2 monomers are average degree of polymerization (DP) times higher than those for linear analog prepared from AB monomers. The number of reactive aromatic carboxylic acids for the hyperbranched polymers is increased as polymerization proceeded. For example, the average number of B groups for the case of hyperbranched polymer prepared from AB_2 monomers is equal to $DP + 1$ when we exclude side reactions. On the other hand, it is always one for linear one from AB monomers. Regardless what average DP of linear analog, it has only one reactive carboxylic acid at one end when they are synthesized from AB monomer. Single hyperbranched polymer molecule could also form multiple links to CNT due to numerous functional groups are available. Thus, the covalent attachment of hyperbranched PEK to the CNT would most likely result in hyperbranched PEK grafted to CNT (HPEK-*g*-CNT) nanocomposites.

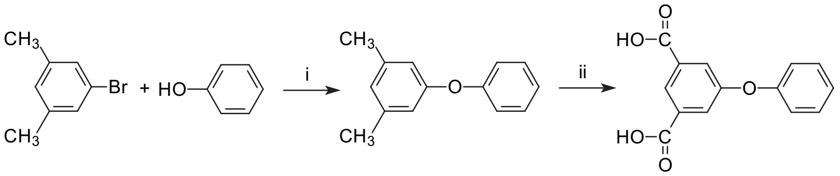

1 **2**

Fig. 1. Synthesis of 5-phenoxyisophthalic acid (**2**): (i) KOH, Cu, DMF; (ii) $KMnO_4$, H_2O/pyridine.

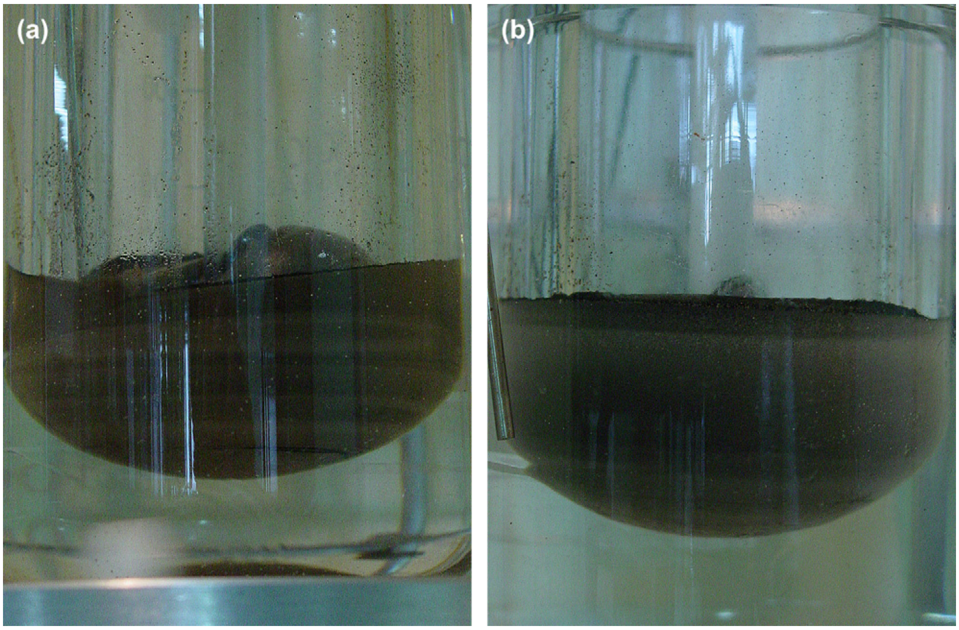

Fig. 3. Digital photographs of the reaction mixtures: (a) hyperbranched PEK-*g*-SWNT and (b) hyperbranched PEK-*g*-MWNT.

The resultant nanocomposites are homogeneously dispersed in various common polar aprotic solvents such as *N*,*N*-dimethylformamide (DMF), *N*,*N*-dimethylacetamide (DMAc), methyl sulfoxide (DMSO), and *N*-methyl-2-pyrrolidinone (NMP). They are even soluble in concentrated aqueous ammonium hydroxide solution. The overall solubility is higher than 1 wt% (10 g/Kg), and thus, the nanocomposites could be potentially very useful in the field of CNT research to achieve substantial solubility in common organic solvents. Thus, they are potentially very valuable for further applications.

The carbon and hydrogen contents of nanocomposites obtained from elemental analysis were in good agreement with theoretical values compared to hyperbranched PEK homopolymer (Table 1). However, the carbon contents of all samples are less than the theoretical amounts. This would be originated from the hygroscopic nature of hyperbranched PEK, which contains large number of aromatic carboxylic acids.

3.3. Thermal properties

The DSC samples (powder form) were subjected to two cycles of heating from room temperature to 300 °C and then cooling to room temperature with ramping rate of 10 °C/min (Fig. 4).

In the first heating scan of HPEK-*g*-SWNT (Fig. 4(a)), there was a broad endothermic peak ranged from room temperature to 150 °C with the peak centered at 92.3 °C with 88.0 J/g of heat of evaporation (ΔH_{vap}), which was originated from the heat loss occurred by water evaporation that was uptaken by the hygroscopic property of the sample. As proposed, this would be an explanation for the lower carbon content in elemental analysis (Table 1). The sample displayed T_g at 217.2 and 216.8 °C in the first heating and cooling scans, respectively (Fig. 4(a)). The T_g was 226 °C, which was the same as reported value [48], in the second heating scan. The reason that T_g value was not significantly affected by SWNT's, which could play as nanoscale rigid filler reducing matrix free volume as well as hampering molecular motion, would be there already exist tremendous hydrogen bonding between the numerous number of carboxylic acids on the molecular periphery. As a result, filler effect would not be the major influence, since the T_g value of carboxylic acid-terminated HPEK is already approximately 90 and 76 °C higher than those of corresponding linear *m*PEK and phenoxy-terminated HPEK,

Table 1
Elemental analysis and properties of HPEK-*g*-CNT nanocomposites

Sample	Elemental analysis			DSC			TGA[c]			
		C (%)	H (%)	T_g[a] (°C)	T_{exo}[b] (°C)	ΔH_{exo} (J/g)	In air		In nitrogen	
							$T_{d5\%}$ (°C)	Char at 600 °C (%)	$T_{d5\%}$ (°C)	Char at 600 °C (%)
3a	Calcd.	73.20	2.98	226	92.3	88.0	412	13.5	433	74.2
	Found	72.64	2.99							
3b	Calcd.	73.20	2.98	228	82.9	90.9	442	13.5	441	75.6
	Found	69.94	3.01							

[a] Determined by DSC from the second heating scan with heating rate of 10 °C/min.

[b] Determined by DSC from the first heating scan with heating rate of 10 °C/min.

[c] The temperature at which 5% weight loss ($T_{d5\%}$) occurred on TGA thermogram obtained with heating rate of 10 °C/min.

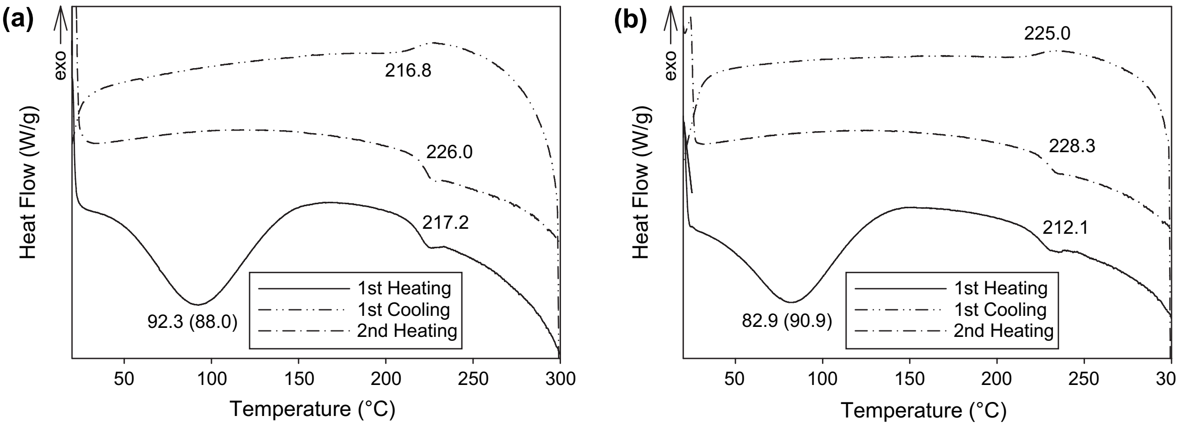

Fig. 4. DSC thermograms of nanocomposites with heating rate of 10 °C/min: (a) hyperbranched PEK-*g*-SWNT and (b) hyperbranched PEK-*g*-MWNT.

whose T_g are about 136 and 150 °C, respectively [38,39,48]. Thus, the T_g increment of HPEK-*g*-SWNT would be solely contributed from hydrogen bonding.

In the case of HPEK-*g*-MWNT, it displayed the glass transition temperature (T_g) at 212 and 225 °C in the first heating and cooling scans, respectively (Fig. 2(b)). The T_g was 228 °C in the second heating scan. Both samples displayed similar thermal behaviors.

The TGA thermograms obtained from both in air and nitrogen are shown in Fig. 5. The 5% weight loss temperatures of purified SWNT were much lower than those of MWNT and they were 361 °C in air and 367 °C in nitrogen. The 5% weight loss temperatures of HPEK-*g*-SWNT were also lower than hyperbranched PEK-*g*-MWNT and they were 412 °C in air and 433 °C in nitrogen. The retention weight percent of the residues at 600 °C was 13.5% in air and 74.2% in nitrogen (Fig. 5(a)). The 5% weight loss temperatures of as-received MWNT were 574 °C in air and 789 °C in nitrogen. For the HPEK-*g*-MWNT sample, they were 442 °C in air and 441 °C in nitrogen. The retention weight percent of the residues at 600 °C in air was 13.5% and in nitrogen was 75.6% (Fig. 5(b)). For both samples, the values of retention weight at 600 °C in air were 13.9 and 13.5%, which agree well with the amount of SWNT and MWNT loads indicating that the reaction medium was less destructive to CNT but strong enough to functionalize CNT. Furthermore, the residual amounts of HPEK-*g*-MWNT at 600 °C were approximately 0.4% in air and 1.4% in nitrogen more than those of HPEK-*g*-SWNT. This would be originated from poorer stability and less purity of SWNT than those of MWNT.

3.4. Scanning electron microscopy (SEM)

Although there are significant amounts of carbonaceous impurities and catalysts are persist in the as-received SWNT, the SEM images obtained from the SWNT treated in PPA at 130 °C displayed much better purity compared to as-received SWNT (purity ∼40%) indicating that impurities such as amorphous carbon beads and metallic catalysts were conspicuously decomposed by heated PPA [49]. From the TGA analysis, it could be confirmed that approximately 83% of impurities were removed. The diameter range of SWNT bundles is 30–45 nm and they are aligned due to applied shear force during the purification process (Fig. 6(a)). In the case of HPEK-*g*-SWNT (Fig. 6(c)), it is noteworthy that diameters of SWNT bundles are in the range of 5–25 nm, which is much smaller than those (40–60 nm) of purified SWNT (Fig. 6(a)). Although SWNT's are still in the bundle state, the average size of bundles is smaller than before grafting of HPEK (Fig. 6(c)) and the shape of them resembles fractal structures. Some

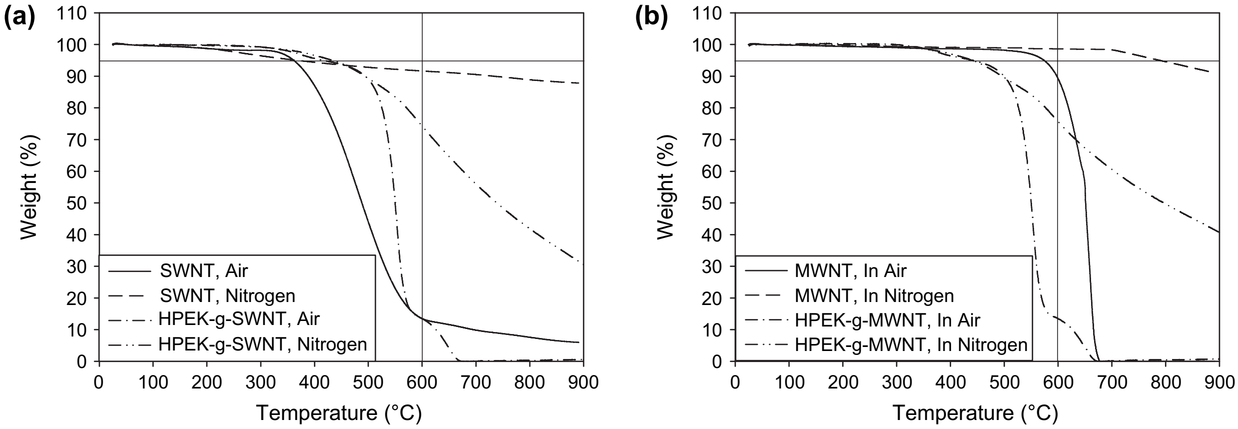

Fig. 5. TGA thermograms obtained with heating rate of 10 °C/min: (a) hyperbranched PEK-*g*-SWNT and (b) hyperbranched PEK-*g*-MWNT.

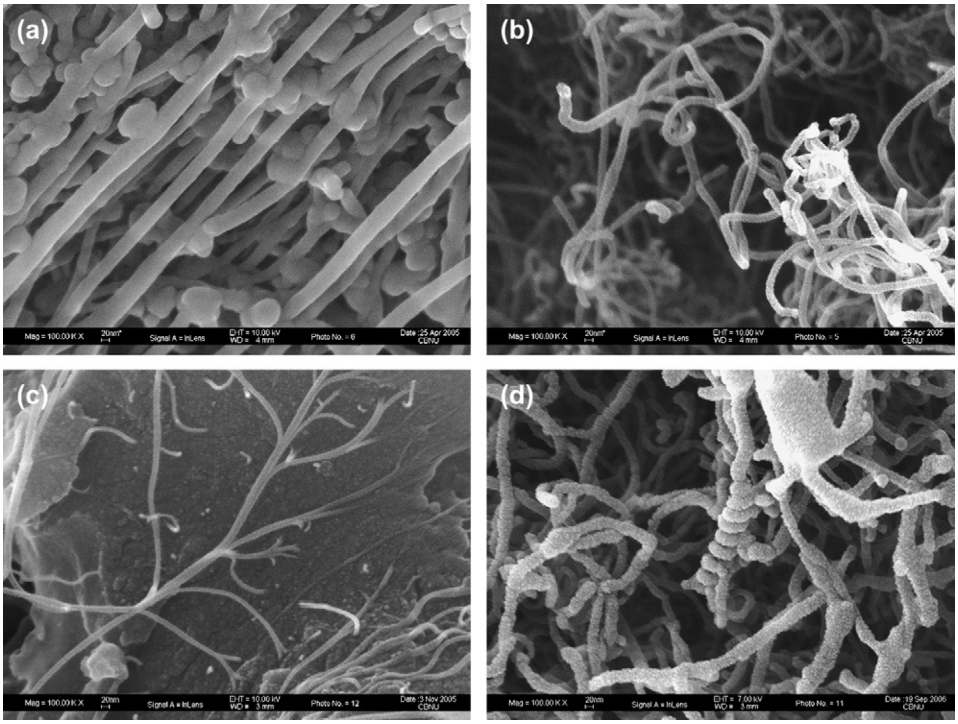

Fig. 6. SEM images of (a) PPA treated SWNT at 130 °C (100,000×); (b) as-received MWNT from Iljin Nanotech Co. (100,000×); (c) hyperbranched PEK-*g*-SWNT (100,000×) and (d) hyperbranched PEK-*g*-MWNT (100,000×).

SWNT fibrils are stemmed out like tree branches and imbedded into hyperbranched matrix. The overall state of dispersion is homogeneous. Thus, it could be hypothesized that the reaction medium, PPA/P_2O_5, plays two important roles to uniform dispersion of SWNT bundles. The one is that PPA is mild enough not to damage SWNT but acidic enough to protonate SWNT, and thus, the tube bundles are homogeneously dispersed into the reaction medium. The other is that both the viscous nature of polymeric acid PPA and strong dehydration power of P_2O_5 cooperatively help to maintain the dispersed state impeding rebundling and functionalization of SWNT bundles, respectively. For instance, once split is occurred at the edge of SWNT bundle when mechanical stirring shear force is applied, viscous polymeric reaction medium containing AB_2 monomer, which is ready to react, is penetrated in between the split and wedged by HPEK. As a result, the splits are started from the tips of SWNT bundles and propagated further into the bundles (Fig. 6(c)). This result suggests that after optimization the potential homogeneous dispersion of individual SWNT could be achieved.

In the case of HPEK-*g*-MWNT, the SEM image of pristine MWNT has been taken for the comparison purpose and it shows that the tube surfaces are seamless and smooth (Fig. 6(b)). After *in situ* polymerization of AB_2 monomer in the presence of MWNT, heavy amount of hyperbranched PEK attached to MWNT could be clearly seen from the SEM image (Fig. 6(d)). The resultant HPEK-*g*-MWNT has the diameter range of 40–150 nm, which is a strong indication that the hyperbranched PEK's are covalently attached to the surface of MWNT. Furthermore, the surfaces of nanocomposites are appeared to be puppy and bumpy compared to pristine MWNT (Fig. 6(b)). The coil-type MWNT (in the middle of Fig. 6(d)) demonstrates that hyperbranched PEK's are attached along the axis of MWNT, which provides further assurance of uniform grafting of HPEK to the surface of MWNT.

4. Conclusion

In situ polymerizations of an AB_2 monomer, 5-phenoxyisophthalic acid, in the presence of carbon nanotubes (SWNT and MWNT) were carried out in PPA/P_2O_5 medium. On the basis of the data from solubility, elemental analysis (EA), thermogravimetric analysis (TGA), as well as scanning electron microscopy (SEM) provided clear evidences for grafting of hyperbranched polymers onto the surface of CNT. The benefits of the reaction condition were further assured that the reaction medium was indeed less destructive to CNT's and powerful enough to graft HPEK onto the surface of CNT's. The resultant HPEK-*g*-CNT nanocomposites have a large number of surface carboxylic acid groups, which is potentially valuable for application-specific-purposes such as polyelectrolyte solutions for Li-ion rechargeable batteries after substitution of acidic protons in carboxylic acid with Li ions, reinforcing additives for the advanced composites taking advantage of enhanced solubility, and etc. Those applications are being investigated.

Acknowledgements

We are grateful to Jeong Hee Lee of Chungbuk National University for conducting SEM. This project was supported by funding from US Air Force Office of Scientific Research, Asian Office of Aerospace R&D (AFOSR-AOARD) and Korea Research Foundation (KRF-2004-D00228).

References

[1] Baughman RH, Zakhidov AA, de Heer WA. Science 2002;297:787.

[2] Shaffer MSP, Fan X, Windle AH. Carbon 1998;36:1603.

[3] Cai L, Bahr JL, Yao Y, Tour JM. Chem Mater 2002;14:4235.

[4] Mickelson ET, Huffman CB, Rinzler AG, Smalley RE, Hauge RH, Margrave JL. Chem Phys Lett 1998;296:188.

[5] Bahr JL, Yang J, Kosynkin DV, Bronikowski MJ, Smalley RE, Tour JMJ. Am Chem Soc 2001;123:6536.

[6] Bahr JL, Tour JM. Chem Mater 2001;13:3823.

[7] Mitchell CA, Bahr JL, Arepalli S, Tour JM, Krishnamoorti R. Macromolecules 2002;35:8825.

[8] An L, Xu W, Rajagopalan S, Wang C, Wang H, Fan Y, et al. Adv Mater 2004;16:2036.

[9] Thostenson ET, Karandikar PG, Chou T-W. J Phys D Appl Phys 2005;38:3962.

[10] Cha SI, Kim KT, Lee KT, Mo CB, Hong SH. Scripta Mater 2005;53:793.

[11] Cha SI, Kim KT, Arshad SN, Mo CB, Hong SH. Adv Mater 2005;17:1377.

[12] Zhang WD, Shen L, Phang IY, Liu T. Macromolecules 2004;37:256.

[13] Liu T, Phang IY, Shen L, Chow SY, Zhang WD. Macromolecules 2004;37:7214.

[14] Andrews R, Jacques D, Rao AM, Rantell T, Derbyshire F, Chen Y, et al. Appl Phys Lett 1999;75:1329.

[15] Qian D, Dickey EC, Andrews R, Rantell T. Appl Phys Lett 2000;76:2868.

[16] Shaffer MSP, Windle AH. Adv Mater 1999;11:937.

[17] Zin L, Bower C, Zhou O. Appl Phys Lett 1998;73:1197.

[18] Haggenmueller R, Gommans HH, Rinzler AG, Fischer JE, Winey KI. Chem Phys Lett 2000;330:219.

[19] Chen GZ, Shaffer MSP, Coleby D, Dixon G, Zhou W, Fray DJ, et al. Adv Mater 2000;12:522;
Dupire M, Michel J. European Patent 1,054,036A1, November 22, 2000.

[20] Sandler J, Shaffer MSP, Prasse T, Bauhofer W, Schulte K, Windle AH. Polymer 1999;40:5967.

[21] Part C, Ounaies Z, Watson KA, Crooks RE, Smith Jr J, Lowther SE, et al. Chem Phys Lett 2002;364:303.

[22] Sun Y-P, Fu K, Lin Y, Huang W. Acc Chem Res 2002;35:1096.

[23] Dai L, Mau WH. Adv Mater 2001;13:899.

[24] Hirsch A. Angew Chem Int Ed 2002;41:1853.

[25] Banerjee S, Kahn MGC, Wong SS. Chem Eur J 2003;9:1898.

[26] Tasis D, Tagmatarchis N, Georgakilas V, Prato M. Chem Eur J 2003;9:4000.

[27] Lin Y, Zhou B, Shiral Fernando KA, Liu P, Allard LF, Sun Y-P. Macromolecules 2003;36:7199.

[28] Huang W, Lin Y, Taylor S, Gaillard J, Rao AM, Sun Y-P. Nano Lett 2002;2:231.

[29] Kumar S, Dang TD, Arnold FE, Bhattacharyya AR, Min BG, Zhang X, et al. Macromolecules 2002;35:9039.

[30] Heller DA, Barone PW, Strano MS. Carbon 2005;43:651.

[31] Zhang T, Shi Z, Gu Z, Iijima S. Carbon 2000;38:2055.

[32] Monthioux M, Smith BW, Burteaux B, Claye A, Fischer JE, Luzzi DE. Carbon 2001;39:1251.

[33] Salzmann CG, Llewellyn SA, Tobias G, Ward MAH, Huh Y, Green MLH. Adv Mater 2007;19:883.

[34] Kim YH. J Polym Sci Part A Polym Chem 1998;36:1685.

[35] Malmström E, Hult A. J Macromol Sci-Rev Macromol Chem Phys 1997;37:555.

[36] Voit B. J Polym Sci Part A Polym Chem 2000;38:2505.

[37] Jikei M, Kakimoto M. Prog Polym Sci 2001;26:1233 [and references therein].

[38] Baek J-B, Tan L-S. Polymer 2003;44:4135.

[39] Choi J-Y, Tan L-S, Baek J-B. Macromolecules 2006;39:9057–63.

[40] Baek J-B, Lyons CB, Tan L-S. J Mater Chem 2004;14:2052.

[41] Baek J-B, Lyons CB, Tan L-S. Macromolecules 2004;37:8278.

[42] Lee H-J, Oh S-J, Choi J-Y, Kim JW, Han J, Tan L-S, et al. Chem Mater 2005;17:5057.

[43] Oh S-J, Lee H-J, Keum D-K, Lee S-W, Park S-Y, Tan L-S, et al. Polymer 2006;47:1132.

[44] Wang DH, Baek J-B, Tan L-S. Mater Sci Eng B 2006;132:103.

[45] Choi J-Y, Oh S-J, Lee H-J, Wang DH, Tan L-S, Baek J-B. Macromolecules 2007;40:4474–80.

[46] http://www.iljinnanotech.co.kr.

[47] Shu C-F, Leu C-M. Macromolecules 1999;32:100.

[48] Shu C-F, Leu C-M, Huang F-Y. Polymer 1999;40:6591.

[49] Han S-W, Oh S-J, Tan L-S, Baek J-B. Polym Prepr 2006;47(2):436.